Timothy M. Hansen *received his B.S. degree in Computer Engineering from the Milwaukee School of Engineering in 2011. He is currently a Ph.D. candidate in the Department of Electrical and Computer Engineering at Colorado State University, working in the Robust Computing and Advanced Power Engineering Laboratory groups. His research interests include robust resource allocation and optimization applied to cyber-physical-social systems in the areas of power engineering and high-performance computing.*

Siddharth Suryanarayanan *is an Associate Professor in the Department of Electrical and Computer Engineering at Colorado State University, where he teaches and performs research in the area of advanced electric power systems. He obtained a Ph.D. in Electrical Engineering from Arizona State University in 2004.*

Anthony A. Maciejewski *is Professor and Department Head of Electrical and Computer Engineering at Colorado State University. From 1988 to 2001 he was a professor of Electrical and Computer Engineering at Purdue University. He holds a Ph.D. from Ohio State University. His research interests include robotics and high performance computing.*

Howard Jay ("H.J.") Siegel *has been the Abell Endowed Chair Distinguished Professor of Electrical and Computer Engineering at Colorado State University since 2001, where he is also a Professor of Computer Science. From 1976 to 2001, he was a professor at Purdue University. He holds a Ph.D. from Princeton University. He has coauthored over 420 technical papers. His research interests include robust energy-aware resource management for heterogeneous parallel and distributed computing, the smart grid for electricity, parallel algorithms, parallel machine interconnection networks, and reconfigurable parallel computer systems.*

Arun V. Modali *received a B.Tech degree in Electrical and Electronics Engineering from Vardhaman College of Engineering, India, in 2012, and an M.S. degree in Electrical Engineering from Colorado State University in May 2014. His research interests include visualization and load flow analyses in the area of power engineering.*

This work is supported by the National Science Foundation (NSF) under grant number CNS-0905399, and by the Colorado State University George T. Abell Endowment.

CrossMark

A Visualization Aid for Demand Response Studies in the Smart Grid

With the influx of data in the emerging smart grid due to technologies such as smart meters and demand response programs, it is more difficult to analyze and discover relevant and interesting information. Using visualization methods for quantifying and comparing the effectiveness and profitability of a given set of solutions to a demand response problem, it becomes possible to answer: whether or not the demand response plan worked effectively, at what times the demand response resulted in a profit or a loss, and, how multiple demand response solutions compare.

Timothy M. Hansen, Siddharth Suryanarayanan, Anthony A. Maciejewski, Howard Jay Siegel and Arun V. Modali

I. Introduction

Each day, power systems engineers are inundated with information. As smart grid technologies such as smart meters and demand response (**DR**) programs evolve and become more widely implemented, the amount of data available will increase drastically (Farhangi, 2010). The abundance of data and information available makes it difficult to assess the state of power systems in a fast and user-friendly manner (Weber and Overbye, 2000). In the field of visualization, it is known that as

  http://dx.doi.org/10.1016/j.tej.2015.03.008

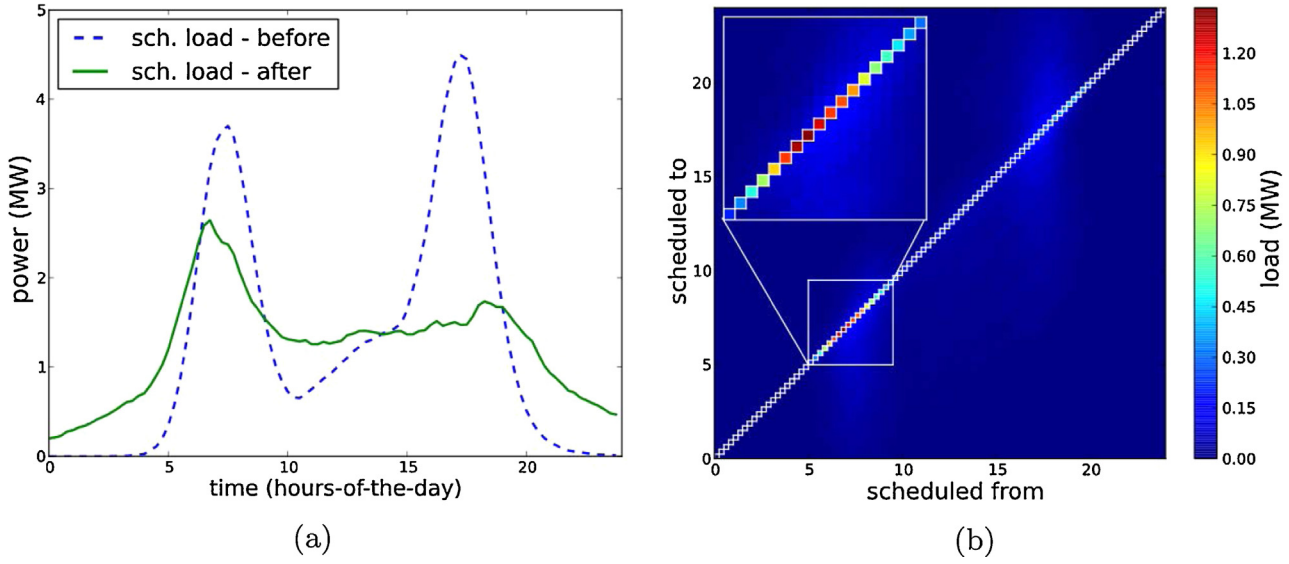

Figure 1: (a) Load Curves of the Schedulable Load Before and After the DR Action in the System in the Constrained Case. A Significant Portion of the Peak Load is Moved to Off-Peak Hours in a Valley-Filling Manner. This Is A Common Way to Present DR Results. (b) A Heat Map Showing The Temporal Source and Destination of the Schedulable Load in the Constrained Case. The Grayscale Shading of a Given Point at Position (x, y) Indicates The Load Moved From Time x to Time y, as Represented by the Accompanying Color Bar. The Black Box Diagonal, i.e., $x = y$, Indicates The Amount of Load That Was Not Rescheduled. If You Sum All Loads At A Given x-Value Across All y in (b), The Total Load Will Equal The Load At the Same x-Value on the Dotted Line in (a). Similarly, The Sum of Load Across All x Will Equal The Solid Line. To highlight the Fact That the Magnitude of the Load That is *Not Moved* From Time 5–9 is Much greater than the Typical Amount of Load *moved* From Any Other Time x to Time y in (b), It is Shown in Greater Detail

the amount of data increases, it becomes more difficult to sift through the data to find key information and present it clearly (Card, 1999). By using proper information visualization techniques, it becomes easier for humans to recognize patterns and analyze information (Ware, 2012). These facts, in part, led to the United States Department of Energy to recognize the importance of visualization in power systems (United States Department of Energy, 2008). Our work attempts to address these issues in the form of new visualization techniques for DR programs.

The economic benefit of small reductions in peak load through DR programs is well understood (Osborne and Warrier, 2007; Albadi and El-Saadany, 2008). One method of DR that is currently being researched is an aggregator-based method that implements centralized control of many smaller-rated loads whose aggregation enables a noticeable change on the load profile of the power system (Hansen et al., 2015; Quinn et al., 2012; Gkatzikis et al., 2013). We use data involving the DR action of 56,642 aggregated small-rated appliances from (Hansen et al., 2015) to design new visualization techniques. The visualization techniques enable a better understanding of the effectiveness of the aggregator-based demand response method. The effect of DR programs is commonly shown as the difference in load curves (Hansen et al., 2015; Logenthiran et al., 2012). A standard representation of a DR load curve is given in Figures 1(a) and 2(a). We believe that this presentation of the data has some limitations, leading to our objective to develop user-friendly visualization tools for quantifying and comparing the effectiveness, the profitability, and the schedule for a given set of solutions to a demand response problem both temporally and spatially.

In the past, work on power system visualization has focused on ''quick-look'' information about the system in the form of graphic overlays on one-line diagrams. This includes spatial contours for visualizing power system voltage data

1040-6190/ http://dx.doi.org/10.1016/j.tej.2015.03.008

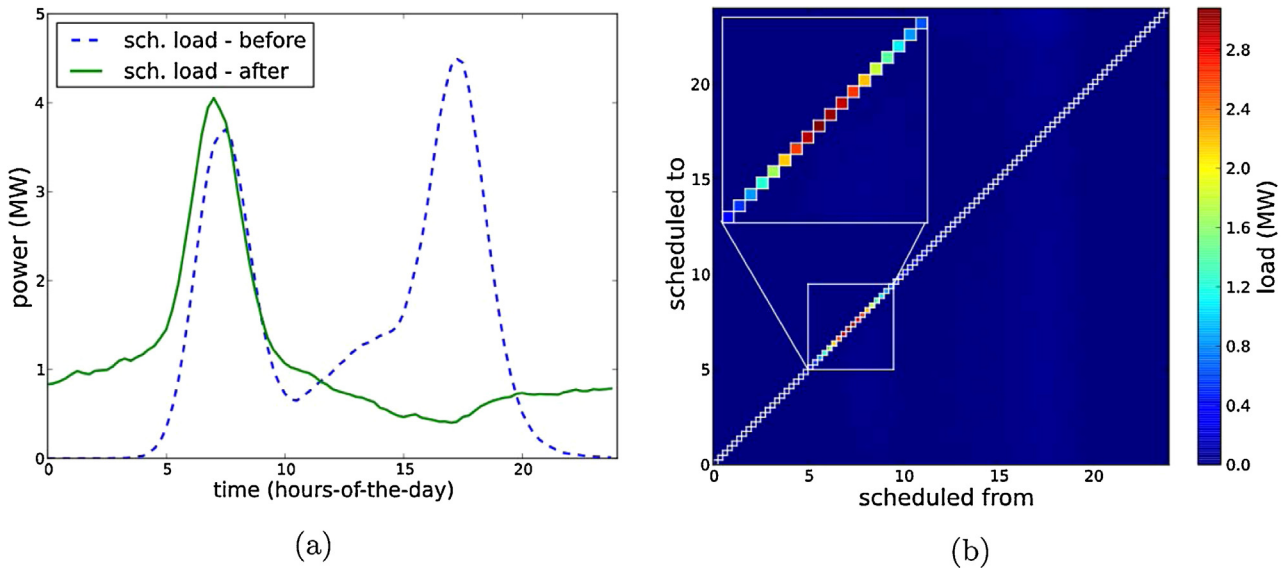

Figure 2: (a) Load Curves of the Schedulable Load Before and After the DR Action in the System in the Unconstrained Case. (b) A Heat Map Showing the Temporal Source and Destination of the Unconstrained Schedulable Load. To Highlight the Fact That the Magnitude of the Load That is *Not Moved* From Time 5–9 is Much Greater Than the Typical Amount of Load *Moved* From Any Other Time *x* to Time *y* in (b), It Is Shown in Greater Detail

(Weber and Overbye, 2000), contingency analysis data (Sun and Overbye, 2004), market power assessment (Overbye et al., 2001), and power flows (Overbye et al., 1995; Glover et al., 2011). Other research on spatial visualizations of power systems has employed geographic information systems (GIS). In Zhang et al. (2010), the contours of real-time voltage magnitude and phase angle measurements, obtained from phasor measurement units, were overlaid on top of the contiguous United States. A neighborhood of photovoltaic (PV) arrays in Anatolia, Calif., and their real-time output were graphically overlaid on the Google Earth geographic area of Anatolia in (Bank and Hambrick, 2013). The power-flow software PowerWorld allows the mapping of voltage contours and network flow information onto maps and exporting this to Google Earth. As far as the authors are aware, no work has occurred to provide the same type of easy-to-understand information for DR programs. This makes it difficult to understand the large quantities of data created by DR programs to determine the effectiveness of the response. With regard to policymakers and other non-technical entities, it becomes more difficult to clearly explain the benefits of DR programs. In that regard, we have designed three new visualization techniques that, at a glance, can provide more information about a set of DR solutions to both system operators and non-technical entities. The first two new techniques provide another temporal dimension of information without obfuscating the graph. The third technique adds a spatial component using GIS in addition to the temporal dimension.

The following contributions are made in this article:

(a) The design and description of two new temporal visualization techniques for a given set of solutions to a demand response problem that answer the following:

(i) Did the demand response plan work effectively?

(ii) When did the demand response entity (aggregator in our work) record a profit or loss?

(iii) How does the difference between the forecast and actual price of the spot market affect the profit margin of the demand response entity?

(b) The creation of a spatial visualization of demand response using GIS that answers *where* in the distribution system did the demand response plan affect load.

  http://dx.doi.org/10.1016/j.tej.2015.03.008

(c) A discussion of how the visualization methods can be used to analyze the effectiveness of demand response optimization techniques.

The remainder of the article is organized as follows. The system model and associated data are provided in Section II. In Section III, the visualization techniques are described and analyzed. Concluding remarks are discussed in Section IV.

II. System Model

According to Roozbehani et al. (2012), by increasing DR technologies and directly allowing retail customers to access the wholesale market, the price elasticity of demand may increase, leading to an increased level of volatility in power systems. An aggregator, which is an intermediary entity that offers the coordination of many entities centrally (Hansen et al., 2015; Quinn et al., 2012), is an alternative to uncontrolled DR (Hansen et al., 2015). Additionally, according to the California Energy Commission (**CEC**), residential loads are not easily controlled and, to provide a strategically useful DR product, need to be composed of a large portfolio of assets (California Energy Commission, 2013).

Our work in Hansen et al. (2015) directly addresses the concerns of the CEC where the aggregator is presented as a for-profit entity that coordinates the schedule of a set of smart appliances belonging to a set of customers and brings the aggregated DR to the market. To encourage customer participation with the aggregator and to offset the inconvenience of a rescheduled appliance, a *customer incentive pricing* structure was proposed. The customer incentive price is a time-varying electricity rate structure that offers the customer a competitive rate of electricity, as determined by the aggregator, for those appliances they allow to be rescheduled as part of the DR action. If the rate is not worth the inconvenience of rescheduling the appliance, the customer is allowed to refuse the aggregator and instead pay the utility company real-time price for electricity (i.e., the status quo) at each time interval for each appliance in the DR. The aggregator-based residential DR program, denoted as Smart Grid Resource Allocation in (Hansen et al., 2015), is formulated as an optimization problem where the objective function is to maximize the aggregator profit. The decisions the aggregator can make in order to maximize profit are the customer incentive pricing and the smart appliance schedule.

Let $\boldsymbol{N}$ be the *income received* by the aggregator for selling negative load to the spot market at the times the smart appliances were *rescheduled from*, $\boldsymbol{S}$ be the *income received* by the aggregator for selling electricity to the customer at the customer incentive price at the times the smart appliances were *scheduled to*, and be the *cost paid* by the aggregator for buying electricity from the spot market at the times the smart appliances were *scheduled to*. The aggregator profit, denoted as $\boldsymbol{P}$, is given by (1).

$$\boldsymbol{P} = \boldsymbol{N} + \boldsymbol{S} - \boldsymbol{B} \tag{1}$$

The optimization was implemented in the form of a genetic algorithm in Hansen et al. (2015) based on a heuristic framework presented in Hansen et al. (2012). The simulation from Hansen et al. (2015) used a probabilistic method adapted from Roche (2012) to generate 56,642 total smart appliances, among 5,555 customers, to be scheduled. The visualization methods presented in this article use the data from the results of the genetic algorithm optimization of these smart appliances and customer incentive pricing (Hansen et al., 2015). For comparison, there are two sets of data: one that is constrained on where loads can be rescheduled to and one that is unconstrained.

To map customers to a spatial location on the distribution network, we use the Roy Billinton Test System (RBTS) (Billinton and Jonnavithula, 1996). The RBTS is a standard six-bus test system with accurately modeled distribution assets that is commonly used for distribution network modeling and simulation (Roche, 2012; Brown et al., 2012; Giraldez et al., 2013). For our simulation purposes, RBTS Bus 5 is modeled, containing 26 loadpoints along four feeders for the 5,555

http://dx.doi.org/10.1016/j.tej.2015.03.008

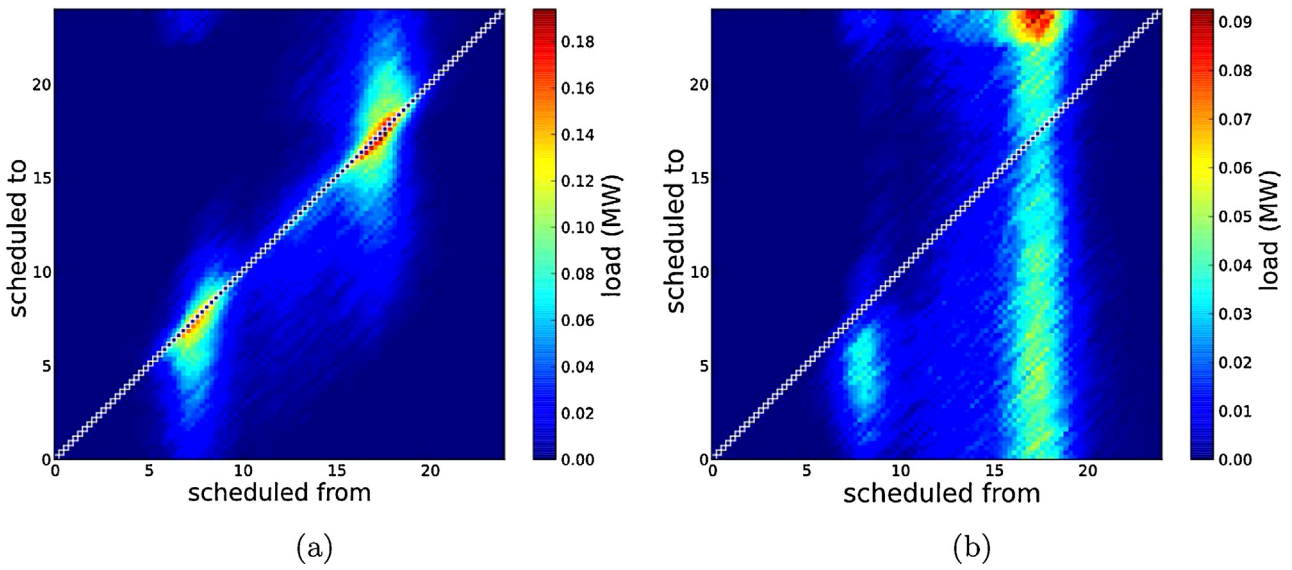

Figure 3: Heat Maps Showing Only the Load That was Moved (So the Diagonal, by Definition, is zero) for (a) The Constrained DR in **Figure 1**(b); and (b) the Unconstrained DR in **Figure 2**(b). In General, The Magnitudes of Points in (b) are Lower Than The Corresponding Points in (a), As Indicated by the Labels on Each Color Bar

customers. The customers are probabilistically assigned to the loadpoints according to the probabilities in **Table A.1**. The probabilities were calculated by normalizing the number of customers on each load point to the total number of customers provided in (Billinton and Jonnavithula, 1996). The nodes in the bus were mapped onto Fort Collins, Colo., using the power line lengths described in the RBTS (the node coordinates are described in Table A.1). The DR from Hansen et al. (2015) was overlaid onto the loadpoints using the same 15-minute intervals over a period of 24-hours, creating a unique spatio-temporal DR visualization.

III. Demand Response Visualization

Demand response actions are usually shown as load data in two dimensions as a load curve, shown in Figures 1(a) and 2(a). Although this provides a glimpse at the aggregate load before and after the DR action, there is information missing about what loads were scheduled when, how much profit was made, the spatial coordination of DR, etc. To overcome the deficiency of this missing information, we propose three additional graph types that have one or more extra dimensions of information. The first is a heat map representation where the x, coordinates indicate the magnitude of the event where smart appliances were rescheduled from time x to time y. The heat map representations can be seen in Figures 1(b), 2(b), 3, and 5. The second type of graph is a three-dimensional (3D) representation where the coordinate (x, y, z) indicates the magnitude z of the DR event where smart appliances were rescheduled from time x to time y, shown in **Figure 4**. The last type of graph represents the DR *spatially* using GIS, as shown in **Figure 7**. The heat maps and 3D load curves were created using the Matplotlib library in Python, with the 3D graphs using the Mplot3d variant. Figures using color-blind-friendly color palettes were also created, although omitted due to space constraints. The GIS figures were created using the Keyhole Markup Language (KML) toolbox in MATLAB to generate overlays for Google Earth.[1]

Figure 1(b) contains the same information as Figure 1(a), but it adds a new dimension of data using grayscale shading as magnitude. Both figures are for the case where the smart appliances have a constraint on what times they can be scheduled to in the DR action. The grayscale shading at the (x, y) coordinate in Figure 1(b) indicates the

 1040-6190/ http://dx.doi.org/10.1016/j.tej.2015.03.008

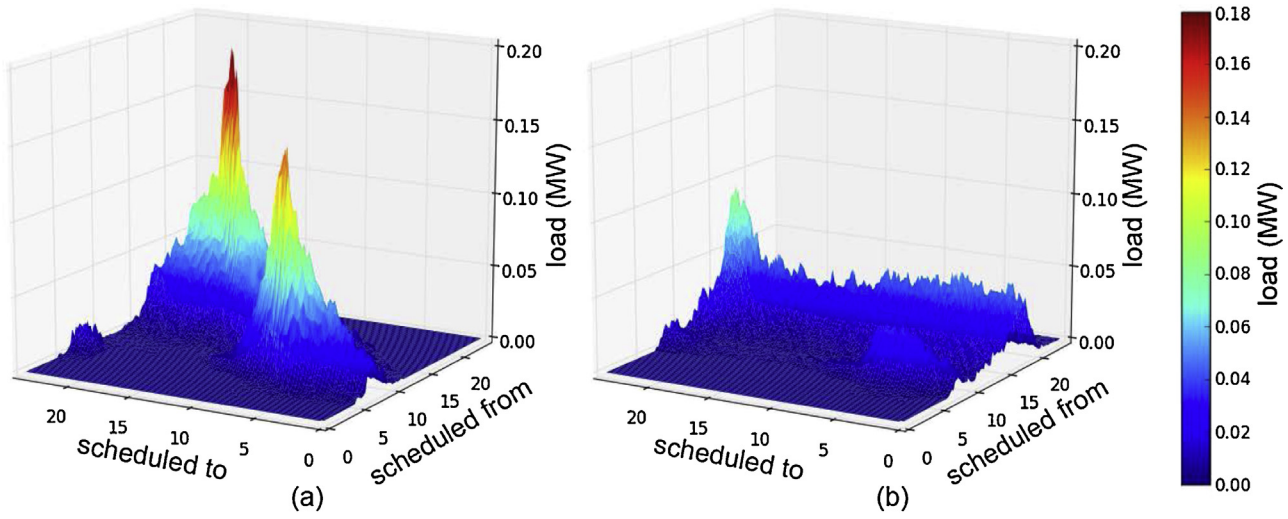

Figure 4: The 3D Load Graph Shows the Temporal Displacement of the Schedulable Loads in Both The (a) Constrained and (b) Unconstrained Cases. Any Point on the Surface (*x*,*y*,*z*) Gives the Load *z*, in MW, Displaced from Time *x* to Time *y*. Graphs (a) and (b) Show the Same Information as **Figures 3**(a) and 3(b), Respectively, But With An Extra Dimension. The Shading Directly Corresponds to the Grayscale Shading and Color Bar in **Figure 3**(a)

magnitude of the load moved from time x to time y. The black squares around the diagonal, i.e., $x = y$, correspond to the amount of load that was not rescheduled. In the case when $x > y$, i.e., below the diagonal, the load was scheduled for a time earlier than originally scheduled. Conversely, a value of $x < y$ indicates the load was scheduled for a later time. At a given original scheduled time of x, the larger the value of $|y - x|$, the further away the load was scheduled via the DR action. Most of the scheduling activity occurs around the peak times, which can be seen in the total schedulable load in Figure 1(a), around 8:00 and 17:00. This is because there is a greater amount of load to be scheduled at those times. Because of the constraint on scheduling times, however, the distance from the original scheduled time is limited, leading to the smaller, but still noticeable, peak observed in Figure 1(a) after the DR action. If you sum all loads at a given x-value across all y in Figure 1(b), the total load will equal the load at the same x-value on the dotted line in Figure 1(a). Similarly, the sum of load across all x will equal the solid line. To highlight the fact that the magnitude of the load that is *not moved* from time 5–9 is much greater than the typical amount of load *moved* from any other time x to time y in Figure 1(b), it is shown in greater detail.

Figure 2 is similar to Figure 1, except it relaxes the constraint on times to which the smart appliances can be rescheduled. This case is used as a comparison of constrained versus unconstrained scheduling. The total electric energy consumed in each heat map is the same (no load shedding), however the relaxation of the constraint on scheduling times leads to a stark difference in the distribution of the load. Figure 2(a) shows that the first peak actually increases the amount of energy consumed. This occurs because in the case that was studied, the spot market and real-time price were lowest during the first peak. This may seem counterintuitive because of the large load at that time, but recall that this is for residential households only and does not take into account commercial and industrial loads. This would most likely change in a residential-heavy distribution area such as that run by ERCOT in Texas, where residential loads during summer account for approximately 50 percent of the total load (Zipperer et al., 2013). To better represent the difference between the load curves in the constrained and unconstrained case in Figures 1(b) and 2(b), respectively, we plot only the load that was moved in Figure 3. The load moved from the second peak is much larger in the unconstrained case and is spread throughout the day. Because of

 1040-6190/ http://dx.doi.org/10.1016/j.tej.2015.03.008

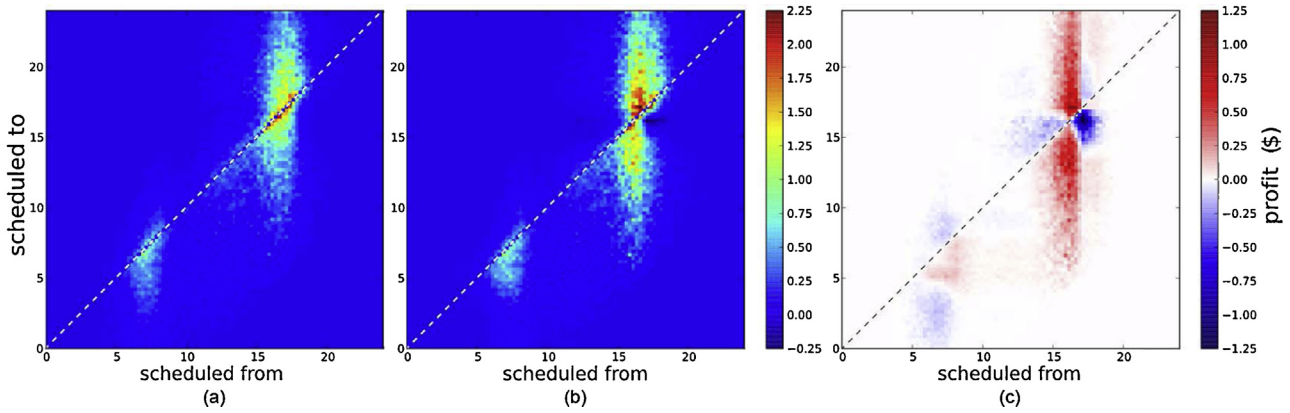

Figure 5: Heat Map of Times That the Aggregator Made a Profit in the Constrained Case. Graph (a) Gives the Aggregator Day-Ahead Forecast Profit When Using Forecast Price Information. In Graph (b), the *Actual* Aggregator Profit is Shown by Replacing the Forecast Information With the Actual Pricing. To Emphasize the Contrast Between Graphs (a) and (b), Graph (c) Shows the Difference Between the Actual Profit and the Forecast Profit (i.e., Actual Minus Forecast). The Grayscale Shading at Position (x,y) on the Heat Map in Graphs (a) and (b) Gives the Profit Made, in USD, From Moving the Loads From Time x to Time y. The Color in Graph (c) Gives the Difference in Profit Between Using the Actual and Forecast Pricing Information, in USD, From Moving the Loads From Time x to Time y. The Darker Areas in (c) Indicate Where the Aggregator Made More Profit Than Forecast, While the Lighter Areas Indicate Less Profit. The Black Dotted Diagonal Line in Graphs (a) and (b), as well as the White Dotted Diagonal Line in Graph (c), Show Where $x = y$

the spreading effect obtained by relaxing the constraint, the magnitude at each data point is lower in Figure 3(b) than in the constrained case in Figure 3(a) (as indicated by the different scales on the color bars).

The same information in Figures 3(a) and (b) can be found in Figures 4(a) and (b), respectively, but with a third dimension. Any point on the surface (x, y, z) gives the load z, in MW, displaced from time x to time y. By using the z-axis in addition to grayscale shading, this presentation of data is better for determining the disparity in magnitude of the schedule at a glance. The shading information directly correlates to the heat map in Figure 3(a). In this presentation, the difference in magnitude between the constrained and unconstrained cases is more apparent than in Figure 3. By relaxing the constraint on what times smart appliances can be scheduled to, there is near uniformity along the *scheduled to* axis around time 20 in Figure 4(b), indicating the magnitude of the appliance loads are near-uniform throughout the day. Because of the magnitude of the load not moved, for presentation purposes, the z values of the four datapoints closest to each $x = y$ datapoint are averaged to create a smooth graph.

The graphs in **Figure 5** are similar to those in Figure 3, but instead of showing load information they show profit information for the constrained case. The grayscale shading at a point (x, y) in Figure 5(a) and (b) shows the profit, in USD, from the smart appliances with start times rescheduled from time x to time y. The black dotted diagonal line shows the times when $x = y$. There is no profit made at these times because the smart appliances were not rescheduled; therefore, there is no income or cost associated. Figure 5(a) shows the profit when calculated using the forecast for both the spot market and real-time price information. The former is obtained from the bulk electricity spot market and the latter is a dynamic pricing scheme from the local distribution company. In our work, we used actual dynamic pricing and spot market pricing data from Saturday, July 9, 2011 (ComEd, 2013; Federal Energy, 2014). This is the data that the aggregator would use for optimization in the day-ahead scheduler. Figure 5(b) shows the profit when the appliance schedule and customer incentive price are evaluated using the actual spot market price. The background color (i.e., when the magnitude is equal to zero) in Figure 5(a) and (b) is lighter than in Figure 3(a) and (b) because the color scale contains negative

  http://dx.doi.org/10.1016/j.tej.2015.03.008

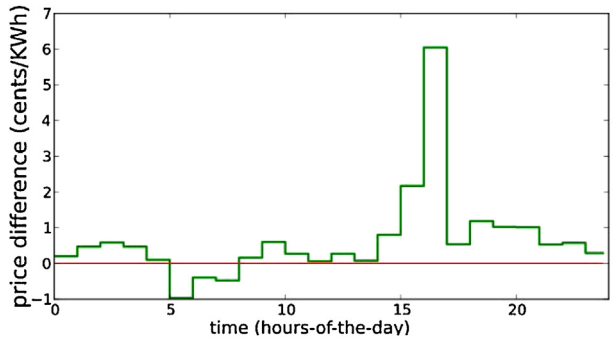

Figure 6: The Price Difference between the Actual and Forecast Spot Market Prices (Federal Energy, 2014) Is Given as the Solid Bold Line. The Light-gray Horizontal Line Indicates No Difference. If The Difference Curves Are Positive, i.e., Above the Horizontal Line, The Price of Electricity Is More Than Forecast. If Negative, The Price of Electricity Is Less Than Forecast

values (i.e., a loss is experienced). Because it can be difficult to pick out the differences between Figure 5(a) and (b), Figure 5(c) shows the *difference* between the actual profit and forecast profit. The grayscale shading at point (x, y) shows the difference in the aggregator profit between using the actual and forecast spot market pricing information from the smart appliances rescheduled from time x to time y. The white dotted diagonal line shows the times when $x = y$. The darker areas show the rescheduling events where the aggregator made more profit than forecast while the lighter areas show those events where less profit was received than expected.

Additional insight into Figure 5(c) is provided by **Figure 6**, which shows the difference in the spot market price between the actual and forecast values. The darker areas in Figure 5(c) are vertically skewed around 16:00, i.e., they correlate to smart appliances scheduled *from* 16:00 to any other time during the day. As shown in Figure 6, this time directly relates to a large increase in the actual spot market price compared to the forecast price. Because these loads are moved *from* these times, they are part of the $\boldsymbol{N}$ term in (1), leading to an increased income from selling these smart appliances as negative loads as part of the DR. Conversely, the lighter areas in Figure 5(c) are horizontally skewed around times 16:00 and vertically skewed around 6:00. The horizontally skewed decrease in profit is due to electricity purchased at a higher spot market price, leading to increased cost from the $\boldsymbol{B}$ term. The vertically skewed profit decrease at time 6 occurs because of a reduction in spot market price, leading to a decreased profit from selling the negative load represented by the $\boldsymbol{N}$ term. The densest areas of white are below the diagonal line, indicating that the smart appliances resulting in this loss were scheduled earlier in the day.

Graph (a) gives the aggregator day-ahead forecast profit when using forecast price information. In graph (b), the *actual* aggregator profit is shown by replacing the forecast information with the actual pricing. To emphasize the contrast between graphs (a) and (b), graph (c) shows the difference between the actual profit and the forecast profit (i.e., actual minus forecast). The grayscale shading at position (x, y) on the heat map in graphs (a) and (b) gives the profit made, in USD, from moving the loads from time x to time y. The color in graph (c) gives the difference in profit between using the actual and forecast pricing information, in USD, from moving the loads from time x to time y. The darker areas in (c) indicate where the aggregator made more profit than forecast, while the lighter areas indicate less profit. The black dotted diagonal line in graphs (a) and (b), as well as the white dotted diagonal line in graph (c), shows where $x = y$.

The plots in Figure 7 show the spatial variation of the DR using GIS overlays. Four figures are displayed to represent the entire 24-hour period, but a time-varying movie can be found with the code at our Web site.[1] The top two figures show the entire RBTS bus and the bottom two figures zoom in on an area of interest. The left two figures show an off-peak time (10:00–10:15) and the right two figures show a peak time (16:45–17:00). The dark black lines show the branches between the

1040-6190/ http://dx.doi.org/10.1016/j.tej.2015.03.008

1040-6190/ http://dx.doi.org/10.1016/j.tej.2015.03.008

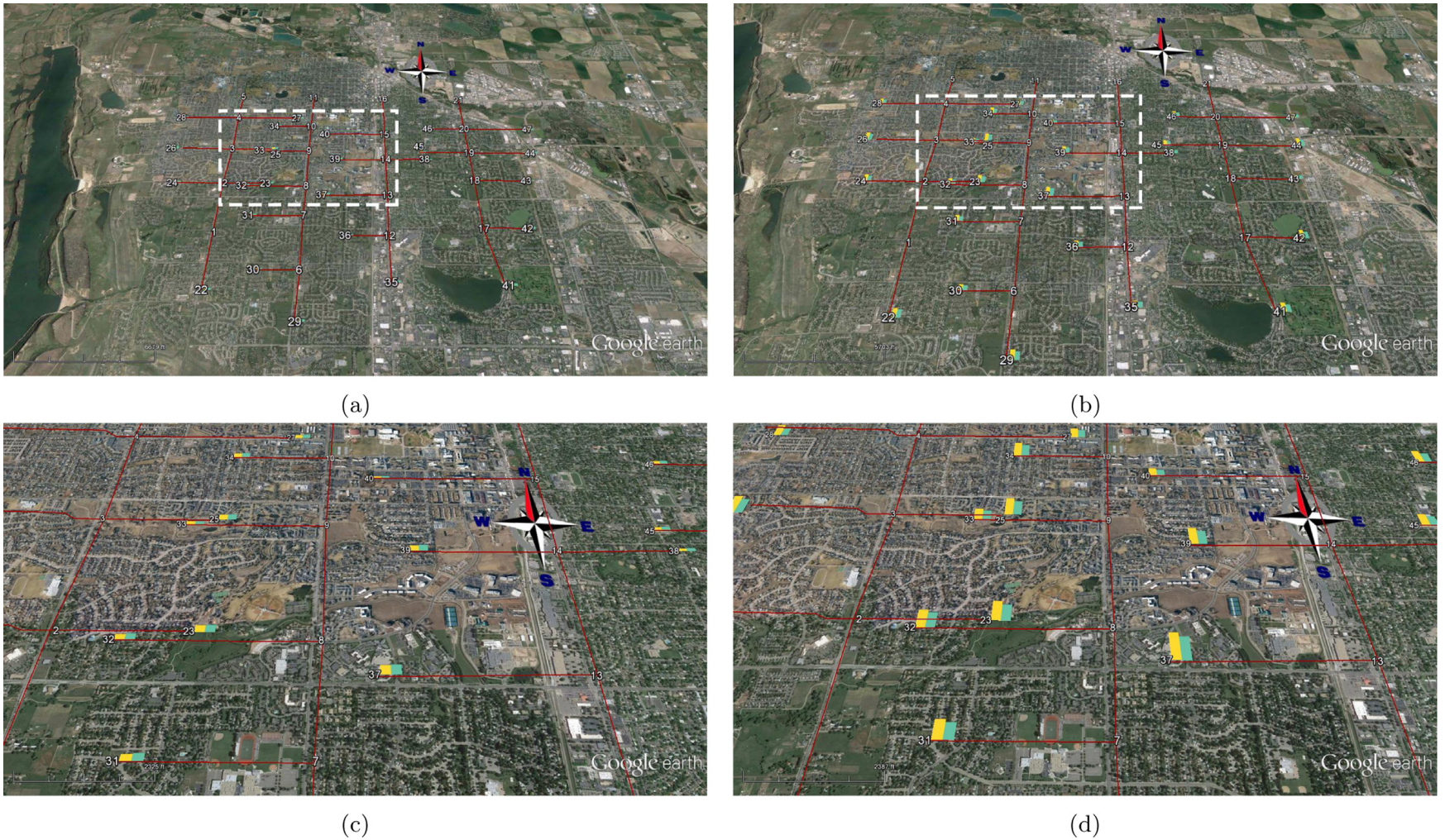

Figure 7: GIS Overlays of a DR Action for the RBTS System Mapped onto Fort Collins, Colorado, in Google Earth. The Top Two Figures Show the Entire RBTS Bus and the Bottom Two Figures Zoom in On An Area of Interest. The Dashed Box in the Top Two Figures Indicate the Zoomed Area of the Bottom Two Figures. The Left Two Figures Show an Off-Peak Time (10:00–10:15) and the Right Two Figures Show a Peak Time (16:45–17:00). The Side-by-Side Bar Graphs Describe the Load Change from the DR Action with the White Bar on the Left Representing the Load Before the DR Action and the Gray Bar on the Right Representing the Load after the DR Action

nodes of the RBTS bus, with the white and black numbers describing the node numbers (GIS coordinates for the nodes are described in Table A.1). The nodes that have the side-by-side bar graphs are the customer loadpoints with the white bar on the left representing the load before the DR action and the gray bar on the right representing the load after the DR action. A scale and compass rose are presented in the bottom-left and top-right corners, respectively, to provide orientation. As shown in Figure 7(d), the DR action is non-uniform in space. Comparing Figure 7(c) to Figure 7(d), the DR action is also non-uniform in time (also shown in the heat maps and 3D load graphs). Without properly mapping the DR information onto a spatial system, such as GIS, these unique spatio-temporal characteristics are lost.

In addition to providing more information to the system operator, these new visualization methods also can help understand how the optimization technique, in our case the genetic algorithm (Hansen et al., 2015), is performing. By examining the load graph in Figures 1(a) and 2(a), one only gets the aggregate information about the load and DR action. The optimization technique, however, makes decisions on individual loads, each with their own initial schedule and constraints. The heat map and 3D graphs help show at a finer grain of detail the decisions being made by the genetic algorithm and their impact on schedules and profits, while the GIS graphs show the spatio-temporal characteristics of the decisions.

IV. Conclusions

Three visualization methods (heat maps, 3D load graphs, and GIS) were adapted for a given set of solutions to a demand response problem. Using these visualization methods, it becomes possible to answer: whether or not the demand response plan worked effectively; at what times the demand response resulted in a profit or a loss; how multiple demand response solutions compare; and where in the distribution system the demand response actions occurred. This allows greater insight into the effectiveness and profitability of the demand

Table A.1: Customer Load Points

Bus	Latitude	Longitude	Bus	Latitude	Longitude	Prob.
1	N40°32′40.10″	W10°56′53.12″	22	N40°31′58.21″	W10°56′53.12″	0.0335
2	N40°33′21.94″	W10°56′53.12″	23	N40°33′21.94″	W10°56′18.77″	0.0434
3	N40°33′55.63″	W10°56′53.12″	24	N40°33′21.94″	W10°57′37.52″	0.0503
4	N40°34′29.15″	W10°56′53.12″	25	N40°33′55.63″	W10°56′18.97″	0.0434
5	N40°34′54.74″	W10°56′53.12″	26	N40°33′55.63″	W10°57′47.86″	0.0503
6	N40°32′12.37″	W10°55′44.32″	27	N40°34′29.15″	W10°55′58.46″	0.0380
7	N40°32′54.00″	W10°55′44.32″	28	N40°34′29.15″	W10°57′47.68″	0.0380
8	N40°33′19.85″	W10°55′44.32″	29	N40°31′38.50″	W10°55′44.32″	0.0353
9	N40°33′53.83″	W10°55′44.32″	30	N40°32′12.37″	W10°56′18.34″	0.0281
10	N40°34′19.89″	W10°55′44.32″	31	N40°32′54.00″	W10°56′28.84″	0.0353
11	N40°34′53.75″	W10°55′44.32″	32	N40°33′19.85″	W10°56′38.85″	0.0353
12	N40°32′38.08″	W10°54′36.43″	33	N40°33′53.83″	W10°56′28.57″	0.0353
13	N40°33′11.69″	W10°54′36.43″	34	N40°34′19.89″	W10°56′18.60″	0.0503
14	N40°33′45.66″	W10°54′36.43″	35	N40°32′4.20″	W10°54′36.43″	0.0281
15	N40°34′11.40″	W10°54′36.43″	36	N40°32′38.01″	W10°55′10.92″	0.0335
16	N40°34′52.93″	W10°54′36.43″	37	N40°33′11.69″	W10°55′30.84″	0.0503
17	N40°32′44.10″	W10°53′21.60″	38	N40°33′45.66″	W10°54′1.92″	0.0281
18	N40°33′25.32″	W10°53′21.60″	39	N40°33′45.66″	W10°55′20.95″	0.0434
19	N40°33′52.33″	W10°53′21.60″	40	N40°34′11.40″	W10°55′31.15″	0.0281
20	N40°34′17.85″	W10°53′21.60″	41	N40°32′2.26″	W10°53′11.60″	0.0353
21	N40°34′51.79″	W10°53′21.60″	42	N40°32′44.18″	W10°52′47.19″	0.0434
			43	N40°33′25.32″	W10°52′37.45″	0.0335
			44	N40°33′52.33″	W10°52′26.82″	0.0503
			45	N40°33′52.33″	W10°54′6.23″	0.0335
			46	N40°34′17.85″	W10°53′55.85″	0.0380
			47	N40°34′17.85″	W10°52′22.90″	0.0380

http://dx.doi.org/10.1016/j.tej.2015.03.008

response programs and the effect of optimizing for the forecast price and data.

The three visualization methods were examined in depth, describing what is being shown and the usefulness of each method. The figures shown here are not exhaustive and represent a subset of the visualization capabilities of the heat map, 3D load graph, and GIS techniques.

Appendix A. Customer Load Points and GIS Data

Table A.1 describes the physical location of each of the numbered nodes from the RBTS bus mapped onto Fort Collins, Colo. (in Figure 7). The coordinates are given in degree-minute-second format. The buses 22–47 are nodes that contain customer loads, with the probability that each of the 5,555 customers exist on a specific node given by ''Prob.'' The buses 1–21 do not contain customer loads and as such do not have an associated probability of containing customers.■

References

Albadi, M.H., El-Saadany, E.F., 2008. A summary of demand response in electricity markets. Electr. Power Syst. Res. 78 (11) 1989–1996.

Bank, J., Hambrick, J., 2013, May. Development of a High Resolution, Real Time, Distribution-level Metering System and Associated Visualization, Modeling, and Data Analysis Functions. National Renewable Energy Laboratory, Golden, CO.

Billinton, R., Jonnavithula, S., 1996. A test system for teaching overall power system reliability assessment. IEEE Trans. Power Syst. 11 (November (4)) 1670–1676.

Brown, H.E., Suryanarayanan, S., Natarajan, S.A., Rajopadhye, S., 2012. Improving reliability of islanded distribution systems with distributed renewable energy resources. IEEE Trans. Smart Grid 3 (December (4)) 2028–2038.

California Energy Commission. 2013 Integrated Energy Report [Online]. Available at: http://www.energy.ca.gov/2013energypolicy/ (accessed 28.03.14).

Card, S.K., 1999. Readings in Information Visualization: Using Vision to Think. Morgan Kaufmann, San Francisco.

ComEd. ComEd residential real-time pricing program [Online]. Available at: https://rrtp.comed.com/live-prices/ (accessed 18.08.13).

Farhangi, H., 2010. The path of the Smart Grid. IEEE Power Energy Mag. 8 (January (1)) 18–28.

Federal Energy Regulatory Commission. PJM daily report archives [Online]. Available at: http://www.ferc.gov/market-oversight/mkt-electric/pjm/pjm-iso-archives.asp (accessed 14.01.14).

Giraldez, J., Roche, R., Suryanarayanan, S., Zimmerle, D., 2013, April. A linear programming methodology to quantify the impact of PHEVs with V2G capabilities on distribution systems. In: 2013 IEEE Green Technologies Conference. pp. 8–15.

Gkatzikis, L., Koutsopoulos, I., Salonidis, T., 2013. The role of aggregators in Smart Grid demand response markets. IEEE J. Sel. Areas Commun. 31 (July (7)) 1247–1257.

Glover, J.D., Sarma, M.S., Overbye, T.J., 2011. Power System Analysis and Design, 5th ed.. Cengage Learning, Stamford, CT.

Hansen, T.M., Roche, R., Suryanarayanan, S., Siegel, H.J., Zimmerle, D., Young, P.M., Maciejewski, A.A., 2012, October. A proposed framework for heuristic approaches to resource allocation in the emerging Smart Grid. In: IEEE PES International Conference on Power Systems Technology (POWERCON 2012), 6 pp.

Hansen, T.M., Roche, R., Suryanarayanan, S., Maciejewski, A.A., Siegel, H.J., 2015. Heuristic optimization for an aggregator-based resource allocation in the Smart Grid. IEEE Trans. Smart Grid, http://dx.doi.org/10.1109/TSG.2015.2399359, 10 pp. (in press).

Logenthiran, T., Srinivasan, D., Shun, T.Z., 2012. Demand side management in Smart Grid using heuristic optimization. IEEE Trans. Smart Grid 3 (September (3)) 1244–1252.

Osborne, J., Warrier, D., 2007, October. A Primer on Demand Response – The Power Grid: Evolving from a Dumb Network to a Smart Grid. Thomas Wiesel Partners Equity Research.

Overbye, T.J., Sauer, P.W., Marzinzik, C.M., Gross, G., 1995. A user-friendly simulation program for teaching power system operations. IEEE Trans. Power Syst. 10 (November (4)) 1725–1733.

Overbye, T.J., Weber, J.D., Patten, K.J., 2001. Analysis and visualization of market power in electric power systems. Decis. Support Syst. 30 (January (3)) 229–241.

Quinn, C., Zimmerle, D., Bradley, T.H., 2012. An evaluation of state-of-charge limitations and actuation signal energy content on plug-in hybrid electric vehicle, vehicle-to-grid reliability, and economics. IEEE Trans. Smart Grid 3 (March (1)) 483–491.

Roche, R., 2012, December. Agent-based Architecture and Algorithms for Energy Management in Smart Grids. (Ph.D. dissertation)Universite de Technologie de Belfort-Montbeliard, Belfort, France.

Roozbehani, M., Dahleh, M.A., Mitter, S.K., 2012. Volatility of power grids under real-time pricing. IEEE Trans. Power Syst. 27 (November (4)) 1926–1940.

Sun, Y., Overbye, T.J., 2004. Visualizations for power system contingency analysis. IEEE Trans. Power Syst. 19 (November (4)) 1859–1866.

United States Department of Energy, 2008, October. 2008 Visualization

Controls and Agenda. Department of Energy Peer Reviews.
Ware, C., 2012. Information Visualization: Perception for Design. Elsevier, Waltham, MA.
Weber, J.D., Overbye, T.J., 2000. Voltage contours for power system visualization. IEEE Trans. Power Syst. 15 (February (1)) 404–409.
Zhang, G., Lee, S., Carroll, R., Zuo, J., Beard, L., Liu, Y., 2010, July. Wide area power system visualization using real-time synchrophasor measurements. In: IEEE Power and Energy Society General Meeting, 7 pp..
Zipperer, A., Aloise-Young, P., Suryanarayanan, S., 2013, September. On the design of a survey for reconciling consumer behaviors with demand response in the smart home. In: North American Power Symposium (NAPS), 6 pp.

Endnote:

1. The datasets, example Python and Matlab GIS graphing code, and color and color-blind-friendly figures may be found at http://www.engr.colostate.edu/sgra/. Questions and comments about the graphing code or datasets can be addressed to the corresponding author.

1040-6190/ http://dx.doi.org/10.1016/j.tej.2015.03.008